
Article:
Li, L., Walkley, B. orcid.org/0000-0003-1069-1362, Reaney, I.M. orcid.org/0000-0003-3893-6544 et al. (1 more author) (2021) The influence of Fe2O3 reagent grade purity on the electrical properties of 'undoped' LaFeO3 ceramics: a cautionary reminder. Journal of the European Ceramic Society, 41 (7). pp. 4189-4198. ISSN 0955-2219

https://doi.org/10.1016/j.jeurceramsoc.2021.02.019

The influence of Fe_2O_3 reagent grade purity on the electrical properties of 'undoped' $LaFeO_3$ ceramics: a cautionary reminder.

Linhao Li*[1], Brant Walkley[2], Ian M Reaney[1] and Derek C. Sinclair[1]

[1] Department of Materials Science and Engineering, University of Sheffield, Mappin Street, Sheffield, S1 3JD, UK

[2] Department of Chemical and Biological Engineering, University of Sheffield, Mappin Street, Sheffield, S1 3JD, UK

Abstract

Low levels of impurities can have a dramatic influence on the electrical properties of metal oxides. Here, we use a combination of impedance spectroscopy and Seebeck coefficient measurements to show the defect chemistry and p-type conduction mechanism in undoped $LaFeO_3$(LF) ceramics is significantly influenced by impurities in Fe_2O_3 reagents. A low but significant concentration of impurities associated with 99.9% Fe_2O_3 reagent is sufficient to compete against the intrinsic Schottky disorder responsible for the p-type behaviour normally observed for undoped LF ceramics. This produces electrically heterogeneous grain (bulk) responses that are strongly dependent on the processing conditions. To achieve electrically homogeneous bulk responses requires adjustment of the oxygen content by annealing in a reducing atmosphere (n-type) or via doping with a significant level of acceptors (mixed ionic/ p-type electronic). These results illustrate the importance of using high purity reagents when studying the electrical properties of ferrite-based perovskites.

Keywords: lanthanum ferrite, Impedance, conduction mechanism, electrical microstructure, impurity

* Electronic mail: linhao.li@sheffield.ac.uk.

Introduction

Stoichiometry is important in perovskites as it influences the defect chemistry and consequently the electrical properties.[1–6] In some cases, low levels of impurities can have a dramatic effect on the electrical properties. A classic example is the influence of unintentional acceptor-doping in 'undoped' $BaTiO_3$ due to low levels (few hundreds of ppm) of Al^{3+} and Fe^{3+} impurities in TiO_2 reagents used in the formation of the perovskite[6]. This generates a low level of oxygen vacancies that can results in the uptake of oxygen (on cooling) as described by the Kroger-Vink equation below and explains the p-type behaviour observed for 'undoped' $BaTiO_3$ ceramics prepared and measured in air.

$$V_O^{\cdot\cdot} + \frac{1}{2}O_2(g) \rightarrow O_O^{\times} + 2h^{\cdot} \quad (1)$$

Undoped $LaFeO_3$ (LF) is another example where non-stoichiometry plays a key role in the electrical conductivity. Its stoichiometry has long been debated, in particular the level (if any) of La-deficiency, $La_{1-x}FeO_{3-\delta}$. Wærnhus et al [7,8] investigated the electrical properties of LF ceramics at values of x = 0.003 and -0.003 and found them to be independent of composition. Secondary phases in these non-stoichiometric compositions were identified by Transmission Electron Microscopy and the authors inferred a narrow homogeneity range for $La_{1\pm x}FeO_{3-\delta}$ with $x < 0.003$. High temperature isothermal equilibrium conductivity measurements as a function of partial pressure of oxygen, pO_2, showed that at 1000 ºC and $pO_2 < 10^{-12}$atm, n-type behaviour occurs due to oxygen loss associated with the following reaction

$$O_O^{\times} \rightarrow \frac{1}{2}O_2(g) + V_O^{\cdot\cdot} + 2e' \quad (2)$$

that can be interpreted as partial reduction of some Fe^{3+} to Fe^{2+} ions, $La(Fe^{3+}_{1-x}Fe^{2+}_{x})O_{3-\delta}$.

The electrical conductivity, σ, behaviour and defect models above this pO_2 have been the subject of debate with data often being irreproducible on reduction/oxidation cycles and being very temperature, time and grain size dependent. For example, Wærnhus et al [7] report the need for at least 4 days at 1000 ºC for $pO_2 > 10^{-4}$ atm to achieve time independent conductivity values. Through extensive studies of annealing samples either at low or high pO_2 before performing conductivity relaxations at various pO_2 values, Wærnhus et al [7,8] established time independent isothermal conductivity of nominally stoichiometric LF ceramics at 1000 ºC. Three regions of different behaviour were identified on log σ-log pO_2 plots for T= 1000 ºC. In the range 10^{-17} – 10^{-12} atm the slope is -1/6 (n-type) before becoming independent of pO_2 in the intermediate range 10^{-10} to 10^{-7} atm and then switching to a slope of 3/16 (p-type) for $pO_2 > 10^{-4}$ atm. The n-type behaviour is attributed to oxygen loss and therefore mixed Fe^{2+}, Fe^{3+} in LF; the pO_2 (and time) independent behaviour in the intermediate range was attributed to a full oxygen lattice whereby further oxidation could not take place without the formation of new oxygen lattice sites. The p-type behaviour observed > 10^{-4} atm associated with oxidation was attributed to intrinsic Schottky disorder where both cation and anion vacancies are created. Oxidation occurs via filling of these oxygen vacancies and therefore forming '$LaFeO_{3+x}$' (or more correctly, a cation deficient perovskite), The p-type behaviour can be attributed to partial oxidation of Fe^{3+} to Fe^{4+} ions (and/or O^{2-} to O^{-}); however, diffusion of cations (associated with the Schottky disorder) is slow and this is the origin of the time dependent conductivity observed in this region of T-pO_2. Finally, the authors report these Schottky

defects are thermally activated and can be frozen at lower temperatures and therefore conductivity is time independent below 1000 ^{o}C.

A well-established method to enhance p-type behaviour in LF is via A-site acceptor doping with Sr^{2+} ions.[9,10] This has the advantage that the oxygen vacancies created by acceptor doping exceeds that associated with the intrinsic Schottky defects. This allows easy and rapid oxidation of the lattice and results in high levels of p-type conduction to be achieved and reversible conductivity behaviour on reduction and oxidation. Sr-doped LF materials have been used and studied as mixed ionic-electronic conducting cathodes in Solid Oxide Fuel Cells.[11–13] All of these models for undoped and acceptor-doped LF have been substantiated by atomistic calculations.[14–16]

An important (but often neglected) aspect in the synthesis and characterisation of ceramics is the purity of the starting reagents. An excellent example of where this is important to achieve single phase materials is the purity of Fe_2O_3 reagents used in the solid-state synthesis of perovskite $BiFeO_3$ (BF) using Bi_2O_3 and Fe_2O_3. Valant et al[17] have shown the presence of impurities (such as Al) in Fe_2O_3 reagents (99% pure) are sufficient to force the Bi_2O_3 – Fe_2O_3 system into a quasi-ternary system and the nominal composition into a phase field that contains BF, $Bi_{25}FeO_{39}$ and $Bi_2Fe_4O_9$. This results in BF ceramics that contain significant levels of secondary phases. To ensure single phase BF ceramics were obtained Valant et al[17] employed 99.9995% purity Fe_2O_3.

Given the sensitivity of the p-type behaviour to thermally activated Schottky defects in LF it is of interest to consider the influence of the purity of Fe_2O_3 reagents on the electrical properties of LF ceramics. Here we compare LF ceramics prepared in air but made from two different sources (99.9% and 99.998%) and which show very different electrical behaviour. Impedance Spectroscopy (IS) is used to probe the electrical microstructures of the ceramics and Seebeck coefficient measurements to identify p- or n-type behaviour. IS results show LF ceramics prepared from the higher purity Fe_2O_3 yield resolvable bulk and grain boundary responses with conducting grains and insulating grain boundaries. Seebeck coefficient measurements confirm the expected p-type behaviour. In contrast, ceramics prepared from the lower purity Fe_2O_3 reagent give non-ideal impedance responses that are challenging to interpret and contain components that are not reproducible on heating/cooling cycles in air over a modest temperature range, ~ 25 – 400 ^{o}C. Seebeck coefficient measurements suggest n-type behaviour for ceramics sintered in air at 1500 ^{o}C, whereas those sintered at 1350 ^{o}C are p-type below 400 ^{o}C but n-type from 400 -800 ^{o}C. These results are inconsistent with the expected defect chemistry models proposed for LF. Annealing low purity ceramics in 5%H_2 at 500 ^{o}C and remeasuring the IS and Seebeck coefficient gives well resolved bulk and grain boundary responses with n-type behaviour. A-site doping with Sr at 5at% in low purity ceramics gives a bulk response and an electrode response consistent with a mixed ionic-electronic conductor. Seebeck coefficient measurements yield the expected p-type behaviour.

This study demonstrates that the reagent grade of Fe_2O_3 has a significant influence on the measured electrical properties of undoped LF and can be attributed to the low but significant concentration of donor impurities associated with the Fe_2O_3 reagent competing against Schottky disorder responsible for the p-type behaviour normally observed for undoped LF ceramics prepared in air. Homogeneous bulk responses that are consistent with the expected defect chemistry of LF can be achieved using lower purity reagents by either adjusting the oxygen content by annealing in

a reducing atmosphere to attain n-type behaviour or by doping with a significant level of acceptors (e.g., Sr for La) to attain the expected mixed ionic/ p-type electronic behaviour.

Experimental procedure

$LaFeO_{3\pm\delta}$ and $La_{0.95}Sr_{0.05}FeO_{3-\delta}$ ceramics were prepared by the conventional solid-state route. La_2O_3 (99.9%, ,Sigma-Aldrich), Fe_2O_3 powders (99.9%, 99.998% Sigma-Aldrich) and $SrCO_3$ (99%, Sigma-Aldrich) were used as raw materials. Two batches of $LaFeO_{3\pm\delta}$ were prepared, one using 99.9% Fe_2O_3 (denoted LP for Lower Purity $LaFeO_{3\pm\delta}$) and the other with 99.998% (denoted HP for Higher Purity $LaFeO_{3\pm\delta}$). $La_{0.95}Sr_{0.05}FeO_{3-\delta}$ ceramics were prepared using 99.9% Fe_2O_3 and are denoted as LP-Sr. The powders were pre-dried (180 °C for $SrCO_3$, 600 °C for Fe_2O_3 and 900 °C for La_2O_3) for 6 h before weighing in appropriate quantities and then mixed by grinding using an agate mortar and pestle in acetone for 40 min followed by calcination at 1100 °C for 6 h in air. The resultant powders were then ground for another 40 min. Green bodies were first formed by a uniaxial steel die and then isostatically pressed at 200 MPa before sintering in air for 6 h at various temperatures ranging from 1100-1500 °C. A selection of LP $LaFeO_{3\pm\delta}$ ceramics that were sintered in air at 1500 °C were annealed in a tube furnace at 500 °C for 10 hrs in flowing 5 % H_2/95% N_2 gas and will be denoted as LP-H_2. The absolute density of samples was recorded by a combination of geometric and Archimedes' methods. The relative density was obtained using absolute density divided by theoretical density which was calculated from the corresponding atomic weight and lattice parameter.

The crystalline phases were determined by X-ray powder diffraction (XRD) analysis using a Stoe STADI/P transmission system and a Bruker D2 Phaser using $CuK_{\alpha 1}$ radiation on sintered and crushed samples. Lattice parameters were calculated from the XRD patterns based on a Pbnm orthorhombic cell using WinXPow software. A combination of a Philips XL 30S FEG scanning electron microscope with a Noran energy dispersive X-ray analyser (SEM/EDX) was employed to examine the phase purity and microstructure of the sintered ceramics. Samples for SEM were polished and thermally etched at 90% of the sintering temperature for 1 h before being coated with carbon.

Impedance spectroscopy (IS) using an applied voltage of 100 mV was performed using a combination of a Solartron 1260 system and a Solartron Modulab. Au paste (fired at 850 °C for 2 h), Ag paste (fired at 200 °C for 2 h) or In-Ga (applied at room temperature) were used as electrodes to coat on both major faces of ceramics and measured over a temperature range of 100 – 1000 K. Sub-ambient measurements were performed in an Oxford Instruments CCC1104 Closed Cycle Cooler Cryostat and above ambient in air (or flowing 5%H_2/95% N_2 for H_2-annealed ceramics) in an in-house rig that was inserted into a non-inductively wound tube furnace and temperature controlled to ±1°C. IS data were corrected for sample geometry (thickness/area) and, additionally, high frequency data were corrected for instrumental-related inductance by performing a short circuit measurement to assess the lead resistance and associated inductance of our set-up. Seebeck coefficient (S) measurements were performed in air from 300 to 700 °C (Heating rate 5 °C/min, holding until the variation of temperature is less than 0.5 °C/3mins) on bar samples by a conventional steady-state method with a Netzsch SBA 458 Nemesis. The S measurements were performed in Ar

for LP-H_2 and in air for all other samples.

Results

Phase Purity and Ceramic Microstructure

The room temperature (RT) XRD patterns for LP ceramics sintered at different temperatures are shown in Figure 1 (a). The phase purity is clearly dependent on the final sintering temperature. XRD peaks associated with La_2O_3 (space group P321) are observed in samples with lower sintering temperatures (1100 ~ 1200 ^oC) but disappear when the sintering temperature reaches 1350 ^oC. Based on XRD, samples remain phase-pure up to a sintering temperature of 1500 ^oC. RT XRD patterns of LP, HP and LP-Sr ceramics sintered at 1500 ^oC as well as LP after post annealing in 5 % H_2 at 500 ^oC (LP-H_2) are shown in Figure 1(b). All peaks may be attributed to a single perovskite phase based on XRD analysis with similar lattice parameters at RT, Figure 1 (b) insert.

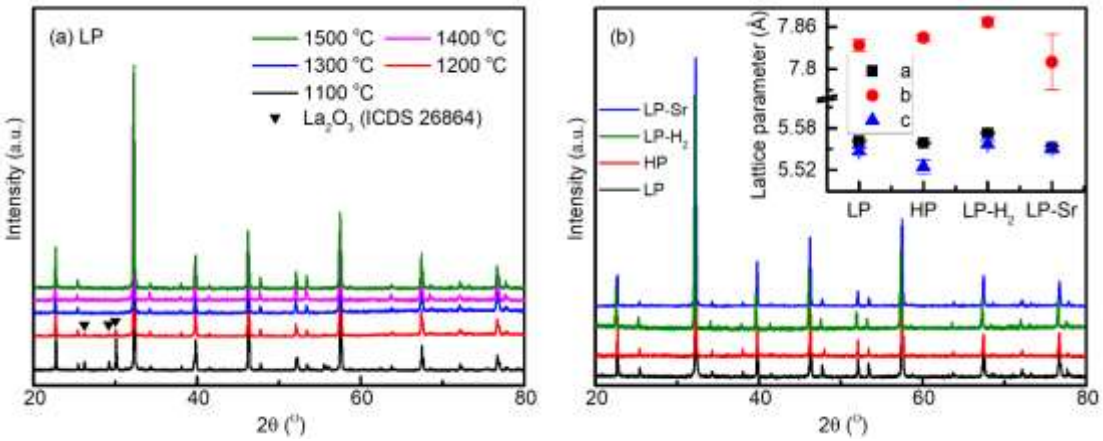

Figure 1. Room temperature X-ray powder diffraction data for (a) LP $LaFeO_3$ ceramics sintered at different temperatures and (b) LP, HP, LP-H_2 and LP-Sr ceramics. Insert in (b) shows the lattice parameters for LP, HP, LP-H_2 and LP-Sr ceramics.

Based on geometric and Archimedes' methods, the density of the ceramics used for electrical characterisation were estimated to be ~ 95, 90, 98 and 95% for LP, HP, LP-Sr and LP-H_2, respectively. SEM results revealed a significant difference in the microstructures of LP, HP and LP-Sr ceramics. The images show a relatively large amount of porosity within HP which agrees with their relative density. LP displayed large grains in the range ~ 10 -100 μm with a more irregular shape whereas HP and LP-Sr had relatively regular grains with much smaller sizes, < 10 μm, Figure 2. The microstructure of LP-H_2 is relatively similar to LP ceramics which indicates no significant change in microstructure occurs from the annealing process. EDX data (Table1) revealed a slightly Fe-deficient La-rich composition compared to the theoretical values. However, the difference between the LP and HP data are rather insignificant and within the standard deviations associated with the measurements.

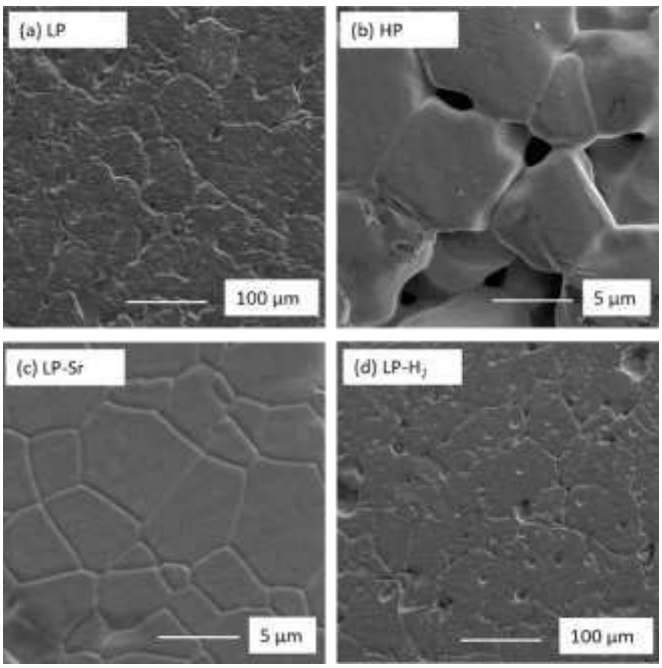

Figure 2. SEM secondary electron images of (a) LP, (b) HP, (c) Sr-doped and (d) H_2 annealed $LaFeO_3$ ceramics.

Table 1. Chemical composition (relative cation at%) and associated error (standard deviation) by SEM/EDX of LP- and HP-$LaFeO_3$ ceramics.

Sample	**Fe (at%)**	**La (at%)**
LP	48.6 (±0.6)	51.4 (±0.6)
HP	48.5 (±0.7)	51.5 (±0.7)

Electrical Properties

Impedance data collected on the ceramics revealed LP-Sr and HP to be semiconducting at RT with total resistivity < 1 MΩcm, whereas LP and LP-H_2 were insulating at RT with total resistivity > 1 MΩcm. Representative complex impedance plane (Z*) plots for the ceramics at various temperatures are shown in Figure 3 and all display either overlapping and broadened arcs (LP and HP Figure 3 (a) and (b)) or evidence of at least two distinct responses (LP-H_2 and LP-Sr Figure 3 (c) and (d)). The total resistivity of each sample, R_{total}, was estimated using the low frequency intercept of the Z* data on the Z' axis. An Arrhenius plot of total conductivity, $\sigma_{total} = 1/ R_{total}$, is summarised in Figure 3 (e) along with the activation energy, E_a, values associated with σ_{total} which are in a range from ~ 0.14 eV (LP-Sr) to 0.68 eV (LP-H_2).

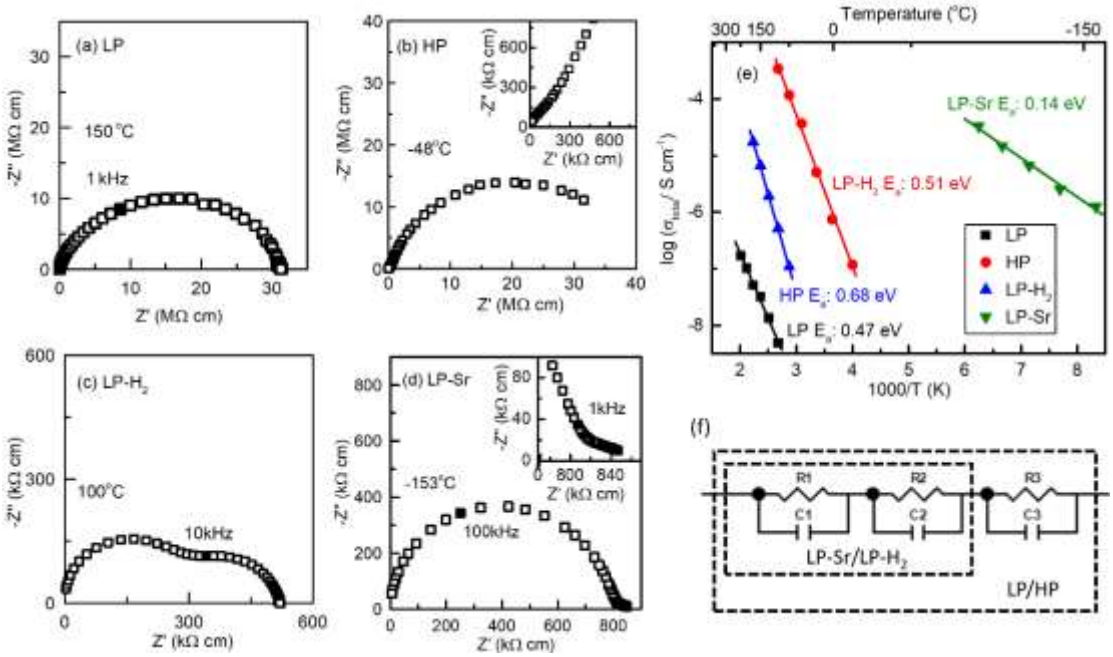

Figure 3. Z* plots for (a) LP at 25°C; (b) HP at -48°C; (c) LP-H_2 at 100°C; (d) LP-Sr at -153°C. (e) Arrhenius plot of total conductivity, σ_{total}, versus reciprocal temperature for LF ceramics. (f) Equivalent circuits used to interpret the impedance data.

To investigate the electrical properties in more detail we used multiformalism IS analysis by using combined spectroscopic plots of (i) the imaginary components of impedance, Z'', and electric Modulus, M'' (Z'', M'' spectra) and (ii) the real component of the complex capacitance (C') and M'', (C', M'' spectra) in conjunction with the Z* plots for all ceramics. This analysis allows identification of the low capacitance grain (bulk) response (typically in the order of ~ pF/cm) based on the presence of a large M'' Debye peak and a low capacitance C' plateau.

For equivalent circuit analysis based on the brickwork layer model for electro-ceramics, single Debye peaks in Z'', M'' spectra (or a single arc in Z* and M*) with maxima that are coincident (or close) in frequency and a low C' plateau in C' spectra are assumed to be a single, parallel Resistor-Capacitor (RC) combination associated with a bulk response.[18,19] The presence of additional M'' and/or Z'' Debye peaks (or arcs in Z* and/or M*) and higher C' plateaus or inclines at lower frequency than the bulk response indicate other electroactive regions such as grain boundaries and/or electrode effects. These are normally assumed to be additional parallel RC elements that are connected in series with the bulk response. In this study, equivalent circuits with 2 (LP-Sr and LP-H_2) or 3 (LP and HP) parallel RC elements connected in series were adopted as shown in Figure 3 (f). M'' spectra that contain large M'' Debye peaks can be used to estimate both capacitance and conductivity using the relationships

$$C = 1/2M'' \tag{3}$$

$$\omega_{max}RC = 1 \tag{4}$$

ω_{max} is the angular frequency at the peak maximum (where $\omega = 2\pi f$, where f is in Hz), C is capacitance and R is resistance (but all corrected for the geometric factor of the ceramic). This type

of analysis is particularly useful for identifying and characterising electrically heterogeneous ceramics based on conductive grains and insulating grain boundaries where the bulk response is not readily accessible from Z* plots (or Z'' spectra) alone; however, R and C can be estimated using M'' data.[18,19] Data using this approach are presented for LP-Sr, HP, LP and LP-H_2 ceramics in Figure 4, 5, 6 and 7, respectively.

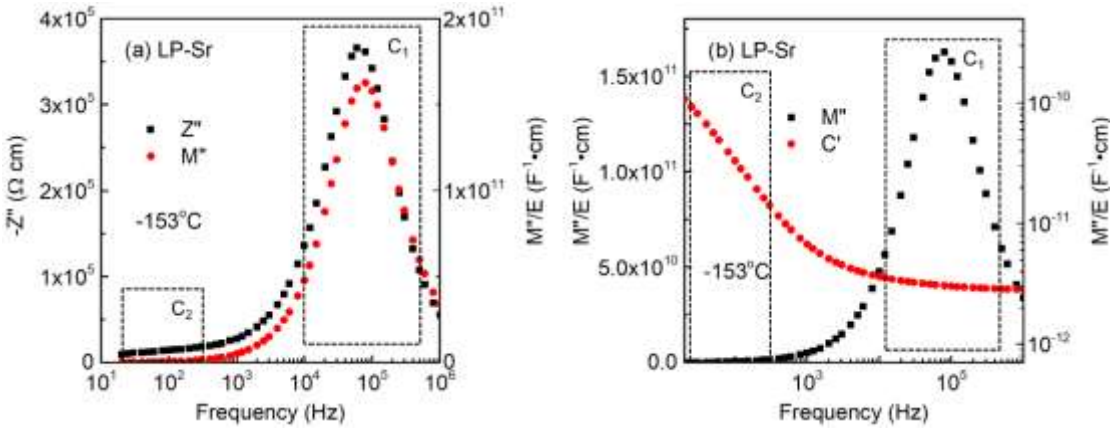

Figure 4. Combined (a) Z'', M'' spectra and (b) C', M'' spectra for LP-Sr ceramic at -153 °C.

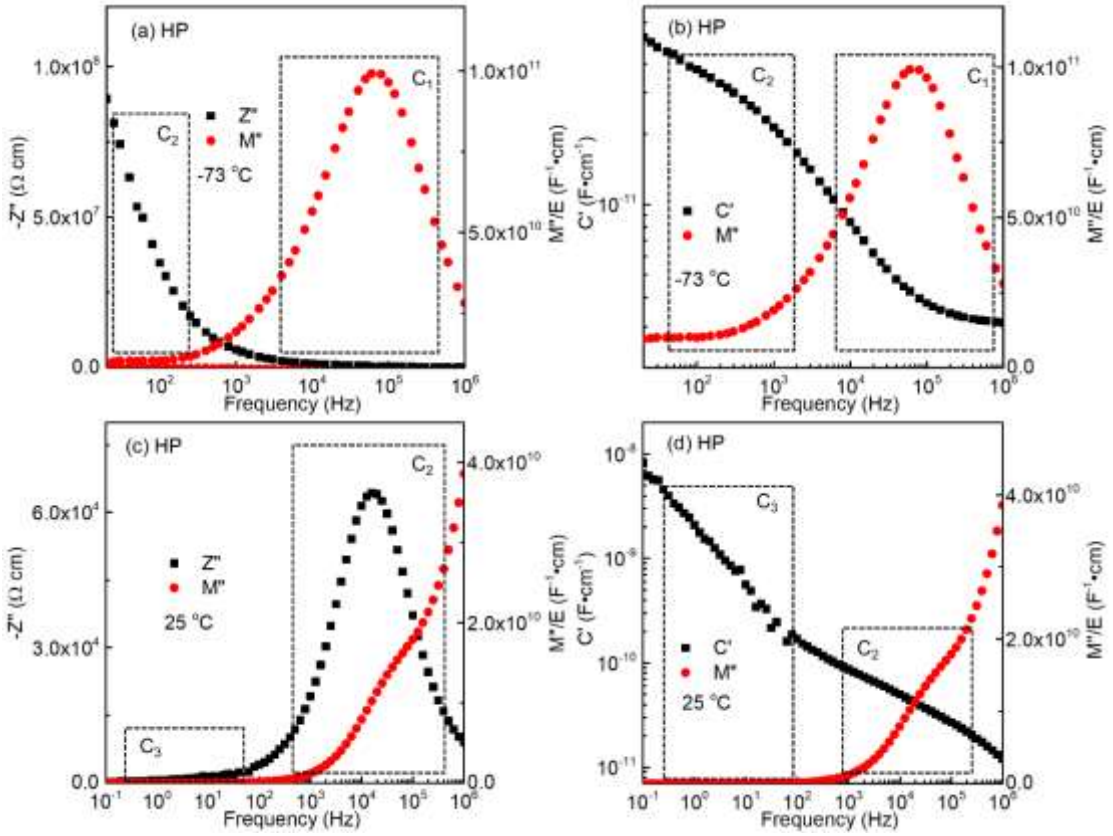

Figure 5. Combined Z'', M'' and C', M'' spectroscopic plots for HP ceramic at (a),(b) -73 °C and (c),(d) 25 °C.

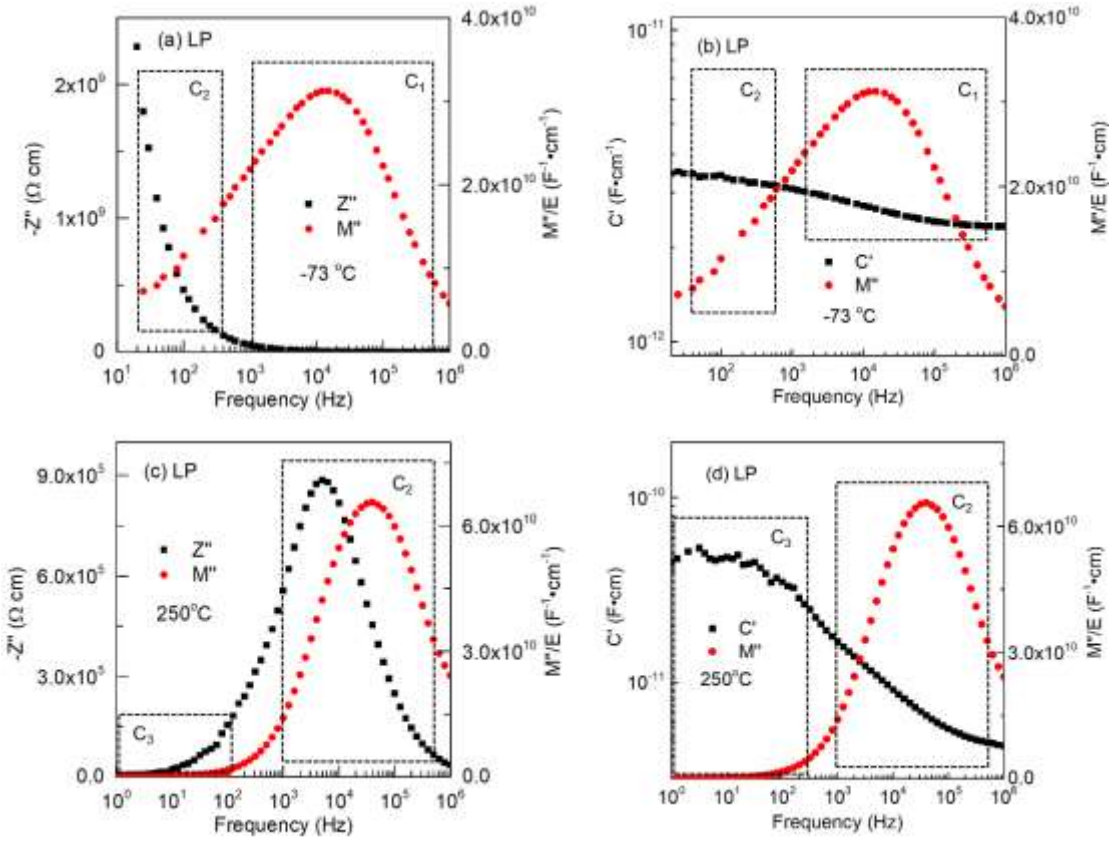

Figure 6. Combined Z", M" and C', M" spectra for LP ceramic at (a),(b) -73 °C and (c),(d) 250 °C.

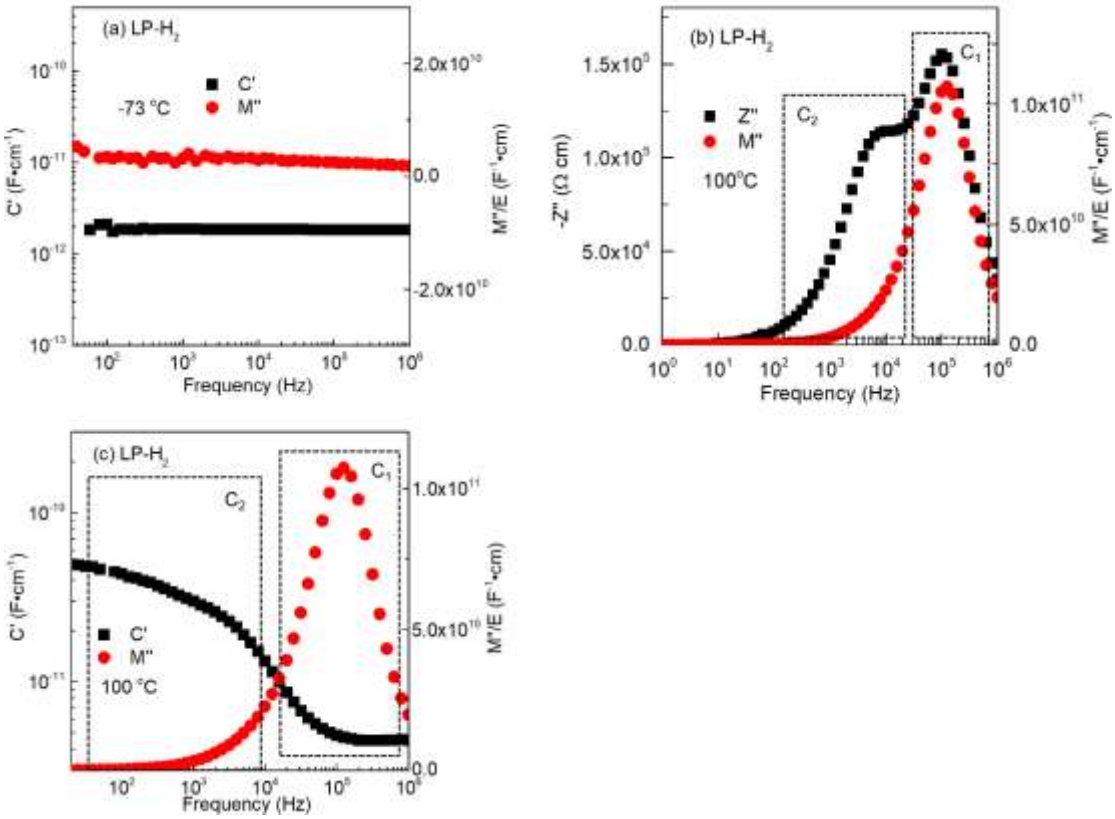

Figure 7. (a) Combined C', M'' spectra at – 73 °C and (b) combined Z'', M'' and (c) C', M'' spectra at 100 °C for LP-H_2 ceramic.

LP-Sr ceramics measured at -153 °C show a single large arc and a low frequency 'tail' in Z* plots, Figure 3 (d), a single M'' Debye peak in the M'' spectrum with ω_{max} similar to that in the corresponding Z'' spectrum, Figure 4 (a) and a low capacitance, high frequency plateau in the C' spectrum with the data rising in magnitude at lower frequency which is consistent with the low frequency tail observed in the corresponding Z* data, Figure 3 (d) inset. To a first approximation the data can be analysed on an equivalent circuit based on two parallel RC elements connected in series, where R_1C_1 models the large Z* arc, Debye peaks in the Z'', M'' spectra and the low capacitance, high frequency C' plateau and R_2C_2 models the low frequency tail in Z* plots and rise in C' data. The magnitudes of C_1 and C_2 are ~ 3 pF/cm and ~ 1 nF/cm, respectively. The former is consistent with a semiconducting bulk (grain) response whereas the latter can be attributed to an electrode effect related to the mixed oxide ion-electronic conductive properties of LP-Sr. An Arrhenius plot of the bulk conductivity ($1/R_1$) for LP-Sr ceramics is shown in Figure 8 with E_a ~ 0.14 eV. Seebeck coefficient, S, measurements of LP-Sr in the range 300 to 700 °C showed S to be ~ + 200 µV/K and therefore p-type, Figure 9.

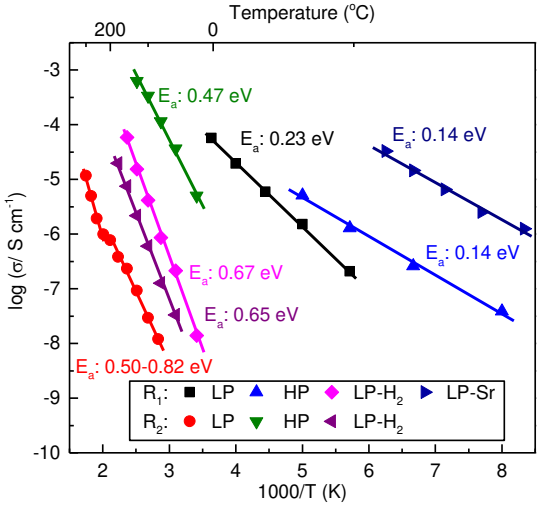

Figure 8. Arrhenius plot of conductivity for R_1 and R_2 in $LaFeO_3$ ceramics.

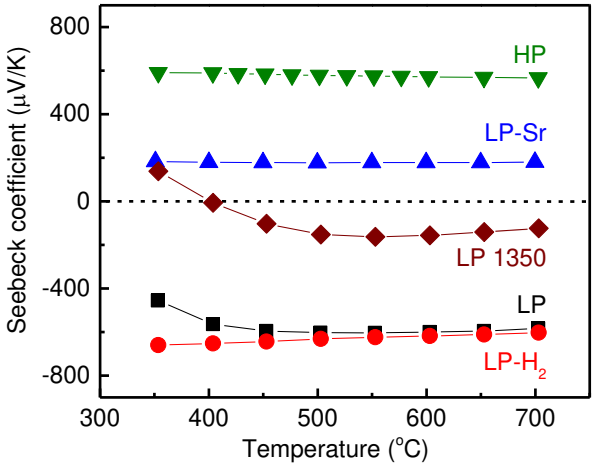

Figure 9. Seebeck coefficient versus temperature for various $LaFeO_3$ ceramics.

Similar to LP-Sr, HP ceramics were semiconducting at RT but with much lower σ_{total} and higher E_a, Figure 3 (e). In this case, the Z* plot for -48 ^oC shows evidence of a small high frequency arc (inset Figure 3 (b)) that is difficult to resolve from a second large arc that dominates the plot, Figure 3 (b). In contrast, Z'', M'' spectra at -73 ^oC show a single M'' Debye peak with C ~ 5 pF/cm and a peak maximum at ~ 10^5 Hz whereas the Z'' spectrum does not show any clear evidence of a Debye peak, instead the Z'' data rise rapidly at low frequency and indicate the presence of a resistive component, Figure 5 (a). The corresponding C', M'' plot shows a C' plateau of ~ 3 pF/cm at high frequency and an inflection towards a second, higher C' plateau with ~ 45 pF/cm, Figure 5 (b). The high frequency M'' peak and low C' plateau are consistent with a semiconducting grain response (R_1C_1). An Arrhenius plot of the bulk conductivity ($1/R_1$) for HP is shown in Figure 8 where the magnitude of the conductivity is two orders of magnitude lower than LP-Sr; however, E_a is the same, ~ 0.14 eV. In this case, S is + 500 V/K and HP are also p-type, Figure 9.

RT spectra provide more information about the additional higher resistive and capacitive electro-active regions present in HP ceramics, Figure 5 (c) and (d). A large Z'' Debye peak with a peak maximum at ~ 20 kHz identifies the presence of a resistive, second RC element with R_2 ~ 120 kΩ/cm and C_2~67 pF/cm. This is confirmed by the presence of a poorly resolved M'' peak at ~ 20 kHz that is swamped by the large M'' incline at high frequency associated with the bulk response (R_1C_1) where the peak maximum now occurs > 1 MHz and therefore outside the measured frequency range, Figure 5 (c). There is a corresponding inflection of C' in this frequency range, Figure 5 (d). The presence of this second element (R_2C_2) is attributed to a resistive grain boundary component associated with the lower density (~ 90%) ceramic microstructure that contains open porosity, Figure 2 (b). An Arrhenius plot of $1/R_2$ is shown in Figure 8 which has an associated E_a of ~ 0.47 eV. The magnitude of the conductivity and associated E_a are similar to that obtained for σ_{total}, see Figure 3 (e). The presence of the large rise in C' at lower frequency indicates the presence of a third RC element with higher capacitance but lower resistance that could not be resolved or quantified from any of the plots but is presumably associated with an electrode effect.

LP ceramic has the lowest σ_{total} of all the ceramics characterised in this study, Figure 3 (e); however, an extremely broad, high frequency Debye-like response was observed in M'' spectra at sub-ambient temperatures, e.g. for – 73^{o}C, Figure 6 (a) and (b), and a total of 3 C' plateaus, 2 M'' Debye peaks and 1 Z'' Debye peak were observed over the range -173 to 300 ^oC, Figure 6. To a first approximation, each of the regions can be associated with a parallel RC element and the elements connected in series. C' spectra at low temperature show the presence of two elements with similar capacitance (labelled C_1 and C_2 in Figure 6 (b) for -73 ^oC) of ~ 2-3 pF/cm, both of which are consistent with grain (bulk) type responses. This is consistent with exceptionally broad M'' peak which has a full width half maximum (FWHM) that exceeds three decades on a log (f) scale. The third element appears at much lower frequency and is only visible at higher temperatures (labelled C_3 in Figure 6 (d) for RT). It possesses a much higher capacitance of ~ 30 pF/cm. The only Z'' Debye peak is associated with C_2, Figure 6 (c), which means among all 3 elements, R_2C_2 is primarily responsible for the distorted arc observed in the Z* plot and therefore dominates the total resistance

of this ceramic, Figure 3 (a), (e) and Figure 6 (d). An Arrhenius plot of $1/R_1$ extracted from the sub-ambient broad M'' peak has lower conductivity than both LP-Sr and HP and has a higher associated E_a of ~0.23 eV. S for LP ceramics sintered at 1500 ºC show a large and negative value of ~ - 550 µV/K which is consistent with n-type as opposed to p-type behaviour, Figure 9.

It is noteworthy that a change in E_a from ~ 0.50 to 0.82 eV was observed for R_2C_2 in LP ceramic around ~200 ºC, Figure 8. To further investigate the origin of this change, LP ceramics were measured on a full heating-cooling IS cycle in air. The heating cycle was measured from 100 to 400 ºC at 25 ºC intervals; the cooling cycle started immediately after the heating cycle and was measured from 400 to 100 ºC at 50 ºC intervals for higher temperatures and at 25 ºC for lower temperatures. A Z* plot measured at 150 ºC on both heating and cooling is shown in Figure 10 (a). The most obvious change is R_{total} (dominated by R_2C_2) decreasing by ~ 1 order of magnitude for measurements taken on cooling compared to that on heating. In contrast, sub-ambient C' and M'' spectra show R_1C_1 remains unchanged during the same heating-cooling cycle, Figure 10 (b). Arrhenius plots of total conductivity from Z* plots of LP on the heating and cooling cycles are given in Figure 11 and show in both cases a significant increase in total conductivity and E_a on the cooling cycle. This data indicates non-equilibrium effects associated with oxidation of LP ceramics during IS measurements at modest temperatures that was not observed in any of the other ceramics. Furthermore, it is noteworthy that LP ceramics sintered at 1350 ºC as opposed to 1500 ºC exhibit a crossover in the sign of S from + to – at 400 ºC indicating a switch from p- to n-type behaviour, Figure 9.

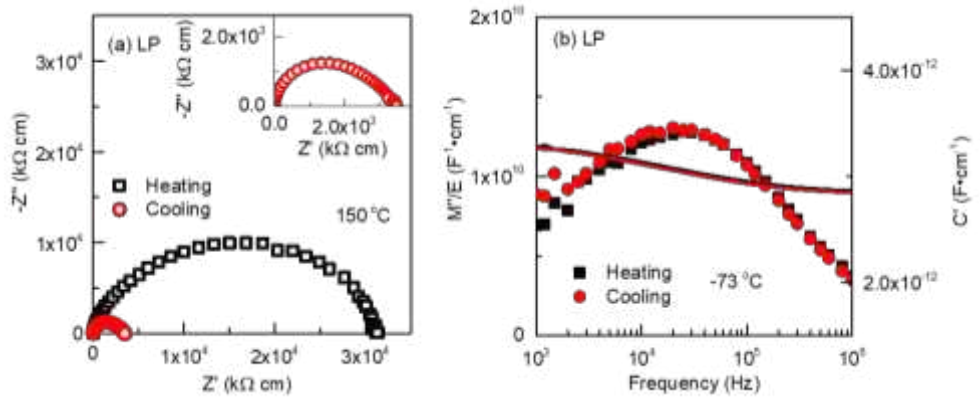

Figure 10. (a) Z* plots for LP on heating and cooling at 150 ºC and (b) C', M'' spectra at -73 ºC on heating and cooling.

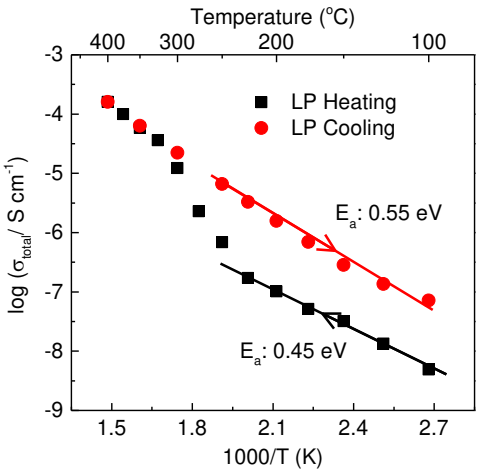

Figure 11. Arrhenius plots of total conductivity for LP ceramics on heating/cooling.

An as-sintered LP ceramic was annealed in 5%H_2-95%N_2 at 500 °C for 10 hours to remove oxygen. To avoid re-oxidation during measurements, the IS response was measured in a flowing 5%H_2-95%N_2 atmosphere. Two well resolved arcs are present in Z* data for LP-H_2 measured at 100 °C, Figure 3 (d) and σ_{total} was at least one order of magnitude higher than LP ceramics sintered in air with a higher E_a of 0.68 eV, Figure 3 (e). Furthermore, there was no sign of any M'' Debye peak associated with a bulk response at sub-ambient temperatures, Figure 7 (a) which is in contrast to the other three samples. A single M'' peak is observed above RT and two Z'' peaks and C' plateaus are observed in spectroscopic plots at 100 °C, Figure 7 (b) and (c), respectively. Thus, within the measured temperature (-173 to 200 °C) and frequency range there are only two RC elements observed for LP-H_2. The extracted capacitance values for these two components are ~ 5 and 30 pF/cm for C_1 and C_2, respectively. Based on the magnitude of capacitance, C_1 is consistent with a grain (bulk) type response; C_2 could be either a grain boundary response or an electrode effect (e.g. non-ohmic contact). In comparison with the two components in LP ceramics where R_1C_1 and R_2C_2 are consistent with grain (bulk) type responses, this indicates the electrical microstructure of LP ceramics become homogeneous after annealing in a reducing atmosphere at a modest temperature of 500 °C.

The conductivity values associated with $1/R_1$ and $1/R_2$ were obtained from the high and low frequency arcs that were easily resolved from Z* plots, Figure 3 (c), and plotted in Arrhenius format, Figure 8. The conductivity and E_a values of $1/R_1$ and $1/R_2$ are relatively similar to each other with E_a ~ 0.66 eV. Compared with the RC elements in LP ceramics their conductivity and E_a are closer to R_2C_2 than R_1C_1. S for LP-H_2 was large and negative in the range of -800 to -600 μV/K indicating n-type behaviour, Figure 9. Changing the electrodes from In/Ga to Au for IS measurements produced an additional low frequency Z* arc and this is attributed to a non-ohmic contact associated with these n-type ceramics, Figure 12. As a consequence, R_2C_2 is attributed to a grain boundary effect as its response remains very similar with both types of electrodes, Figure 12.

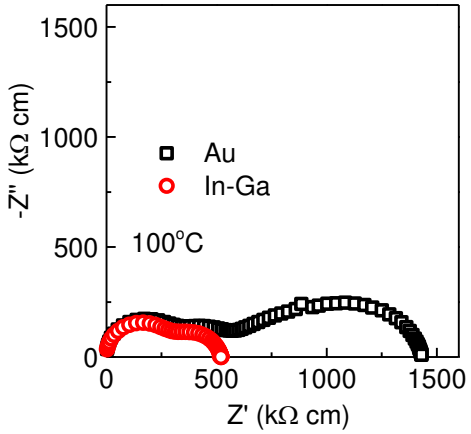

Figure 12. Z* plots for LP with Au and In-Ga electrodes at 100ºC .

Discussion

The purity of the Fe_2O_3 does not have any significant influence on the phase assemblage of the LF ceramics based on laboratory XRD results, Figure 1; however, it does have a significant effect on the microstructures and electrical properties of ceramics prepared using the same processing and sintering conditions. The higher level of impurities in the lower purity Fe_2O_3 reagent results in substantial grain growth with the development of much larger grains (> 10 µm) in LP ceramics with higher density (~ 95%) compared to HP ceramics prepared with the higher purity Fe_2O_3 reagent where the grains are typically < 10 µm and ceramics have lower density (~ 90%), Figure 2.

The electrical properties of the HP ceramics are consistent with that expected based on the existing defect model outlined in the introduction with the creation of intrinsic Schottky disorder above 1000 ºC when processing in air that facilitates uptake of oxygen to fill the anion vacancies created by the Schottky disorder. This results in partial oxidation of Fe^{3+} to Fe^{4+} ions (and/or O^{2-} to O^{-}) in the LF lattice. This gives rise to the electron hopping, Fe^{3+}, Fe^{4+} semiconducting bulk component observed in sub-ambient M'' spectra, Figure 5 (a) and (b), with an associated E_a of ~ 0.14 eV, Figure 8 with S measurements confirming p-type conduction, Figure 9. The 99.998% purity of Fe_2O_3 is sufficient to ensure the level of extrinsic defects due to impurities is below that of the intrinsic Schottky disorder and therefore the measured electrical properties can be rationalised (at least qualitatively) on the intrinsic defect chemistry associated with nominally stoichiometric $LaFeO_3$.

In contrast, the level of impurities in the 99.9% Fe_2O_3 reagent are sufficient to exceed the level of intrinsic Schottky disorder in LP ceramics processed in air and therefore the measured electrical properties are dominated by (unknown) extrinsic, as opposed to intrinsic related defects. Furthermore, the IS data indicate the presence of two, bulk-type responses (R_1C_1 and R_2C_2). The conducting element, R_1C_1, is reversible on heating and cooling in air up to ~ 400 ºC, Figure 10 (a); whereas, the resistive element, R_2C_2, is irreversible on heating and cooling, Figure 10 (a) and Figure

11 and clearly displays non-equilibrium behaviour. Although LP ceramics sintered at 1500 ^{o}C in air exhibit n-type behaviour in the range of 350 to 700 ^{o}C based on their S measurements, those sintered at a lower temperature of 1350 ^{o}C exhibit a p- to n-transition at ~ 400 ^{o}C. It is not possible to establish the electrical microstructure of LP ceramics which contain very large grains with unquantified levels and types of impurities based on the data and analysis presented; however, we discuss two possible scenarios: -

(i) a core (p-type) - shell (n-type) grain structure.

An electrical microstructure based on a conducting p-type core (R_1C_1) and a resistive n-type shell (R_2C_2). The presence of the sub-ambient M'' peak observed for LP ceramics (R_1C_1) is consistent with the semiconducting p-type bulk response observed for HP and LP-Sr ceramics, albeit with a lower level of conductivity and a higher E_a of ~ 0.23 eV, Figure 8. However, the full width half maximum (FWHM) of the M'' peak reaches ~ 3 decades which indicates a high level of heterogeneity in this response, Figure 6 (a), and the higher E_a has a much higher level of uncertainty associated with it based on the crudeness of the ωRC=1 Debye-based calculation on such a non-ideal M'' response. The electrical response of the p-type core (R_1C_1) is reversible on heating and cooling in air between ~ 25 and 400 ^{o}C, Figure 10 (b), whereas the n-type shell (R_2C_2) is more resistive with a higher E_a, Figure 8 and displays irreversible conductivity on the heating and cooling cycles, Figure 11. The n-type behaviour from S measurements indicate these shell-type regions dominate the response in this temperature range. Presumably the n-type electron hopping is associated with mixed Fe^{2+}, Fe^{3+}ions. To explain the increase in conductivity on cooling associated with R_2C_2 during IS measurements requires LP ceramics to irreversibly lose oxygen from the shell regions on heating to 400 ^{o}C.

(ii) impurity donor-doping shifts the p- to n-type transition to higher pO_2.

An electrical microstructure that has been modified due to donor-impurities associated with the lower purity Fe_2O_3 reagent and consists of grains with variable oxygen contents and therefore mixed p- and n-type behaviour. In high purity LF the transition from p-to n-type behaviour requires low pO_2 and high temperature based on equilibrium conductivity data, e.g. < 10^{-12} atm at 1000 ^{o}C.[7] Impurities acting as donor-dopants shift this transition to higher PO_2, and depending on their concentration and distribution lead to further complexities in the equilibrium defect chemistry of LF ceramics. The observed electrical properties are therefore heavily dependent on the ceramic processing conditions (i.e. temperature, time and pO_2) and physical microstructure (i.e. grain size and porosity). This scenario, may explain, in part why LF ceramics sintered at 1500 ^{o}C are n-type based on S measurements whereas those sintered at 1350 ^{o}C display a p- to n-type transition at ~400 ^{o}C, Figure 9. The distribution, level and conductivity of p- and n-type regions in LP ceramics are under thermal kinetic control. The required co-existence of Fe^{2+}/Fe^{3+} (n-type) and Fe^{3+}/Fe^{4+} (p-type) suggests there may be substantial chemical disproportionation of Fe^{3+}ions in LF ceramics.

Although we have been unable to identify an electrical microstructural model to explain the electrical data of LF ceramics we have demonstrated two different methods to dramatically improve electrical homogeneity:

i) Annealing LF ceramics in a reducing atmosphere (5%H_2-95%N_2) results in LP-H_2 ceramics exhibiting a large, temperature stable S ~ -650μV/K indicating n-type conduction, Figure 9. Impedance data for LP-H_2 ceramics displayed only two electrical components attributed to bulk and grain boundary responses, Figure 7 (b). It is noteworthy that the FWHM of the M" peak related to bulk response is ~ 1.23 decades on a log frequency scale which is close to the 1.14 decades based on an ideal Debye response. This demonstrates annealing in H_2 has a dramatic influence on the electrical homogeneity of the grains in LP ceramics and that the electrical microstructure of LP-H_2 ceramics can be based on a simple brick work layer model of grain and grain boundary components connected in series. In this case, the p-type conduction has been completely removed by the annealing process and the ceramics are in the n-type conduction regime.

ii) A modest level (5 at%) of A-site acceptor doping with Sr replacing La is sufficient to compensate for the influence of the impurities in undoped LF ceramics and eliminates the n-type behavior. In this case, LP-Sr ceramics display a positive and temperature stable Seebeck coefficient indicating p-type conduction, Figure 9. Impedance plane plots for LP-Sr consist of a large single arc which represent the bulk response with a low frequency electrode effect associated with the mixed ionic-electronic conduction in these ceramics, Figure 3 (d). The Z", M" and C' spectroscopic data in Figure 4 reveal the grain electrical microstructure of LP-Sr to be reasonably homogeneous with the FWHM of the M" peak associated with the bulk response to be ~ 1.29 decades. This demonstrates that a modest level of A-site acceptor doping is sufficient to create a level of extrinsic oxide vacancies that dominates the defect chemistry. Thus, the influence of the impurities in LP ceramics is compensated and reinstates the p-type electronic conduction in ambient conditions.

Conclusions

The p-type conduction mechanism in undoped $LaFeO_3$ ceramics based on intrinsic Schottky disorder is sensitive to low levels of donor-type impurities that can be present in 99.9% pure Fe_2O_3 reagents used to prepare ceramics by a conventional solid state synthesis route. The grains are electrically heterogeneous and can display co-existence of p- and n-type regions. In contrast, the grain response for ceramics prepared using 99.998% pure Fe_2O_3 were electrically homogeneous and displayed the expected p-type conduction mechanism. To obtain electrically homogeneous grain responses in LF-based ceramics using 99.9% pure Fe_2O_3 reagents requires annealing ceramics in a reducing atmosphere to switch the bulk response to be n-type or to acceptor dope at a modest level to create a sufficient level of anion vacancies to induce mixed ionic/p-type electronic behaviour. This study acts as a pertinent reminder about the importance of using high purity reagents when probing the electrical properties of 'undoped' transition metal perovskite oxides such as $LaFeO_3$.

Acknowledgements

LL, BW, IMR and DCS thank the EPSRC for funding (EP/L027348/1 and EP/L017563/1).

Conflict of Interest

The authors declare no conflict of interest.

References

[1] M. Li, M.J. Pietrowski, R. a De Souza, H. Zhang, I.M. Reaney, S.N. Cook, J.A. Kilner, D.C. Sinclair, A family of oxide ion conductors based on the ferroelectric perovskite $Na_{0.5}Bi_{0.5}TiO_3$, Nat. Mater. 13 (2014) 31–35. https://doi.org/10.1038/nmat3782.

[2] L. Li, M. Li, H. Zhang, I.M. Reaney, D.C. Sinclair, Controlling mixed conductivity in $Na_{1/2}Bi_{1/2}TiO_3$ using A-site non-stoichiometry and Nb-donor doping, J. Mater. Chem. C. 4 (2016) 5779–5786. https://doi.org/10.1039/C6TC01719C.

[3] M. Li, H. Zhang, S.N. Cook, L. Li, J.A. Kilner, I.M. Reaney, D.C. Sinclair, Dramatic Influence of A-Site Nonstoichiometry on the Electrical Conductivity and Conduction Mechanisms in the Perovskite Oxide $Na_{0.5}Bi_{0.5}TiO_3$, Chem. Mater. 27 (2015) 629–634. https://doi.org/10.1021/cm504475k.

[4] S. Aggarwal, R. Ramesh, Point defect chemistry of metal oxide heterostructures, Annu. Rev. Mater. Sci. 28 (1998) 463–499. https://doi.org/10.1146/annurev.matsci.28.1.463.

[5] T. Ikeda, T. Okano, M. Watanabe, A Ternary System PbO-TiO_2-ZrO_2, Jpn. J. Appl. Phys. 1 (1962) 218–222. https://doi.org/10.1143/JJAP.1.218.

[6] N.-H. Chan, R.K. Sharma, D.M. Smyth, Nonstoichiometry in Undoped $BaTiO_3$, J. Am. Ceram. Soc. 64 (1981) 556–562. https://doi.org/10.1111/j.1151-2916.1981.tb10325.x.

[7] I. Wærnhus, P.E. Vullum, R. Holmestad, T. Grande, K. Wiik, Electronic properties of polycrystalline $LaFeO_3$. Part I: Experimental results and the qualitative role of Schottky defects, Solid State Ion. 176 (2005) 2783–2790. https://doi.org/10.1016/j.ssi.2005.08.012.

[8] I. Wærnhus, T. Grande, K. Wiik, Electronic properties of polycrystalline $LaFeO_3$. Part II: Defect modelling including Schottky defects, Solid State Ion. 176 (2005) 2609–2616. https://doi.org/10.1016/j.ssi.2005.07.014.

[9] X.-D. Zhou, Q. Cai, J. Yang, M. Kim, W.B. Yelon, W.J. James, Y.-W. Shin, B.J. Scarfino, H.U. Anderson, Coupled electrical and magnetic properties in (La,Sr)$FeO_{3-\delta}$, J. Appl. Phys. 97 (2005) 10C314. https://doi.org/10.1063/1.1860911.

[10] J. Mizusaki, T. Sasamoto, W.R. Cannon, H.K. Bowen, Electronic Conductivity, Seebeck Coefficient, and Defect Structure of $LaFeO_3$, J. Am. Ceram. Soc. 65 (1982) 363–368. https://doi.org/10.1111/j.1151-2916.1982.tb10485.x.

[11] F. Bidrawn, S. Lee, J.M. Vohs, R.J. Gorte, The Effect of Ca, Sr, and Ba Doping on the Ionic Conductivity and Cathode Performance of $LaFeO_3$, J. Electrochem. Soc. 155 (2008) B660. https://doi.org/10.1149/1.2907431.

[12] T. Ishigaki, S. Yamauchi, K. Kishio, J. Mizusaki, K. Fueki, Diffusion of oxide ion vacancies in perovskite-type oxides, J. Solid State Chem. 73 (1988) 179–187. https://doi.org/10.1016/0022-4596(88)90067-9.

[13] S.P. Simner, J.F. Bonnett, N.L. Canfield, K.D. Meinhardt, J.P. Shelton, V.L. Sprenkle, J.W. Stevenson, Development of lanthanum ferrite SOFC cathodes, J. Power Sources. 113 (2003) 1–10. https://doi.org/10.1016/S0378-7753(02)00455-X.

[14] A. Jones, M.S. Islam, Atomic-Scale Insight into $LaFeO_3$ Perovskite: Defect Nanoclusters and Ion Migration, J. Phys. Chem. C. 112 (2008) 4455–4462. https://doi.org/10.1021/jp710463x.

[15] M. Cherry, M.S. Islam, C.R.A. Catlow, Oxygen Ion Migration in Perovskite-Type Oxides, J.

Solid State Chem. 118 (1995) 125–132. https://doi.org/10.1006/jssc.1995.1320.

[16] F.H. Taylor, J. Buckeridge, C.R.A. Catlow, Defects and Oxide Ion Migration in the Solid Oxide Fuel Cell Cathode Material $LaFeO_3$, Chem. Mater. 28 (2016) 8210–8220. https://doi.org/10.1021/acs.chemmater.6b03048.

[17] M. Valant, A. Axelsson, N. Alford, Peculiarities of a Solid-State Synthesis of Multiferroic Polycrystalline $BiFeO_3$, Chem. Mater. 19 (2007) 5431–5436. https://doi.org/10.1021/cm071730.

[18] J.T.S. Irvine, D.C. Sinclair, A.R. West, Electroceramics: characterization by impedance spectroscopy, Adv. Mater. 2 (1990) 132–138. https://doi.org/10.1002/adma.19900020304.

[19] D.C. Sinclair, A.R. West, Impedance and modulus spectroscopy of semiconducting $BaTiO_3$ showing positive temperature coefficient of resistance, J. Appl. Phys. 66 (1989) 3850–3856. https://doi.org/10.1063/1.344049.